www.springer.com/41230
https://doi.org/10.1007/s41230-022-1159-2

Fabrication and compressive behavior of open-cell aluminum foams via infiltration casting using spherical $CaCl_2$ space-holders

Tan Wan[1], Gang-qiang Liang[1], Zhao-ming Wang[1], Can-xu Zhou[1, 2], and *Yuan Liu[1, 2]

1. School of Materials Science and Engineering, Tsinghua University, Beijing 100084, China

2. Key Laboratory for Advanced Materials Processing Technology, Tsinghua University, Beijing 100084, China

Abstract: The infiltration casting fabrication process based on spherical $CaCl_2$ space-holders and the compressive behavior including the mechanical performance and energy absorption capacity of open-cell aluminum foams were investigated. Open-cell aluminum foams with different porosities in the range of 63.1% to 87.3% can be fabricated by adjusting compression ratios of $CaCl_2$ preforms prepared by precision hot-pressing. The compression tests show that a strain-hardening phenomenon always occurs especially for open-cell aluminum foam with low porosity, resulting in the inclining stress-strain curve in the plateau region. The energy absorption capacity of open-cell aluminum foam decreases with increasing porosity when compared at the same strain. However, when compared at a given stress, each foam can absorb the maximal energy among the five foams in a special stress range. Additionally, open-cell aluminum foam possesses the maximum energy absorption efficiency at its optimum operating stress. At this stress condition, the foam can absorb the highest energy compared with other foams at the same stress point. The optimum operating stress and the corresponding maximal energy absorption decrease with increasing the porosity. The optimum operating stress for energy absorption can also be determined similarly when taking into consideration of the lightweight extent of foams.

Keywords: open-cell aluminum foam; $CaCl_2$ space-holder; infiltration casting; energy absorption

CLC numbers: TG146.21 **Document code:** A **Article ID:** 1672-6421(2022)02-089-10

1 Introduction

Pure aluminum or aluminum alloys' foams (aluminum foams for short) made of solid continuous metallic matrix and massive pores are becoming new kind of engineering materials, which have an attractive combination of structural and functional performance, such as lightweight, high specific strength and stiffness, good energy and sound absorption capacity, and excellent heat transfer and dissipation characteristics [1-3]. Properties of aluminum foams are directly correlated to the corresponding matrix material and the foam structure [4]. Accordingly, the control of the foam structure mainly including pore morphology, pore size and porosity is a research hotspot to achieve optimal performance [5].

Among these fabrication methods for aluminum foams, melt foaming method [6], powder metallurgy method through foaming compacted metal powders mixed with TiH_2 gas releasing agent [7], and gas injection method [8] are for producing closed-cell aluminum foams. In contrast, open-cell aluminum foams are often prepared by the melt infiltration process through filling metal melt into a porous preform which can be removed finally [9, 10]. Generally, two kinds of porous preforms can be used. The first kind of preform is made by filling gypsum slurry into polymeric sponges and roasting the preform to form porous gypsum preform [9]. In this case, the final aluminum foam completely replicates the original structure of the polymeric sponge. So sometimes, this way is also called the investment casting method. The second kind of porous preform is made by compacting the soluble salt particles such as NaCl and $CaCl_2$, etc [10, 11]. In this case, the porous structure of the final aluminum foam replicates the space of the salt particles after being removed by water. So these salt particles are also called space-holders. The melt infiltration method based on the salt space-holder is the most convenient and commonly used method to produce open-cell aluminum foams due to its process

***Yuan Liu**

Male, born in 1974, Ph. D., Associate Professor. His research interests mainly focus on porous metals, alloy solidification foundation and magnetostrictive materials.

E-mail: yuanliu@tsinghua.edu.cn

Received: 2021-08-17; Accepted: 2021-12-21

simplicity, low cost and controllable pore size [12].

Usually, irregularly shaped NaCl particles are the most used space-holders to produce porous preforms because of their lower cost, relatively higher melt point and fast dissolution in water [13]. However, irregularly shaped pores inherited from the NaCl particles will weaken the mechanical properties of aluminum foams [14]. In addition, the final porosity is just in the scope of 60%–70%. It is almost impossible to get porosity higher than 70% because the stacking density of the preform cannot be enhanced due to the poor compressibility of solid NaCl particles even under high-temperature conditions. To solve this problem, Goodall [15] and Chou et al. [16] prepared soft particles such as pyrolized salt and soft ceramic balls as space-holders through the granulation process, which is effective for porosity control but is complicated and time-consuming. In comparison, the industrially produced $CaCl_2$ particles are regular spherical. Recently, Wan et al. [17] found that spherical $CaCl_2$ granules showed obvious deformability at high temperature; therefore, the preform of $CaCl_2$ particles can be compressed into dense packing and a higher porosity of the final aluminum foam can be realized. So the spherical $CaCl_2$ space-holder shows certain advantages in preparing open-cell aluminum foam with higher porosity.

The compressive behavior including both mechanical performance and energy absorption capacity of aluminum foams has been studied by many researchers and is of primary importance in the field of automotive and aerospace, where weight reduction and impact protection are needed to be taken into account [18-20]. Apparently, the compressive behavior of aluminum foam can be efficiently affected by the composition and microstructure of the matrix material and the pore structure, among which porosity is the dominating factor [21, 22].

Gibson and Ashby [23] gave a simple beam model to describe the mechanical performance of aluminum foam:

$$\frac{Y_f}{Y_s} = C \cdot \left(\frac{\rho_f}{\rho_s}\right)^a \quad (1)$$

where Y and ρ are the main mechanical properties and density. Indices of f and s represent the foam and solid. The values of the coefficient a and the structural constant C depend on the foam's structure. Therefore, the realization of precision control of porosity in a wide range is critical to control the mechanical performance of aluminum foams.

The energy absorption capacity of aluminum foam is of particular interest to many researchers [24-26]. It can be measured from the area (shadow region in Fig. 1) at a limiting strain which is typically the densification strain for aluminum foam showing a long plateau region, as shown in Fig. 1(a). However, there is no unified standard to determine the densification strain [27-29]; additionally, it is difficult to find the plateau end at the densification strain especially for those foams with high relative densities. Therefore, the value of energy absorption at the same compressive strain or stress is often used to compare the energy absorption capacity among aluminum foams, as illustrated in Figs. 1(b) and (c). In some protection applications, the strain value of the foams should be restricted below some limit during energy absorption and the energy absorption value is measured at the same strain [30], as shown in Fig. 1(b). Yet, on more occasions, the stress transmitted to the collision point should be controlled within the allowable range and the energy absorption capacity is measured at the same stress, as depicted in Fig. 1(c).

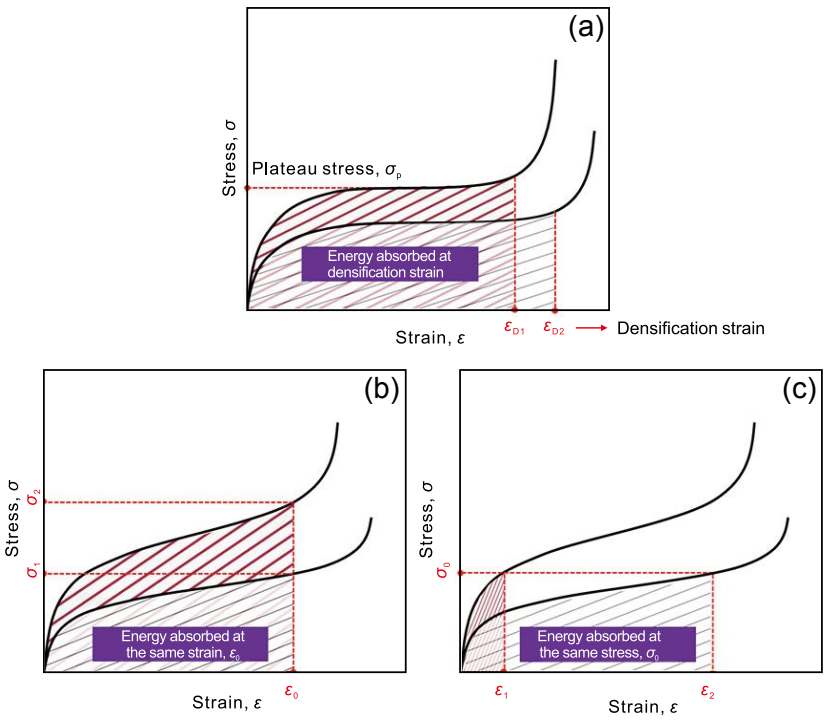

Fig. 1: Schematic illustrations of characterization of energy absorption capacity: (a) energy absorbed at densification strain; (b) energy absorbed at the same strain, ε_0; (c) energy absorbed at the same stress, σ_0

In this study, open-cell aluminum foams with different porosities were fabricated via infiltration technique by using spherical $CaCl_2$ particles as space-holders and ZL102 alloy as matrix materials. A modified hot-pressing method was applied to adjust the packing density of $CaCl_2$ preforms, therefore realizing different porosities of the fabricated aluminum foams. The mechanical behavior of aluminum foams and the corresponding energy absorption characteristics were investigated. Moreover, the energy absorption capacity of aluminum foams was characterized and compared under the same strain and stress conditions, and a design guide for energy absorption application was also presented.

2 Preparation of open-cell aluminum foams

2.1 Materials and fabrication procedures

Spherical $CaCl_2$ particles of mean diameter of 3 mm (purity≥99.5%) supplied by Zhejiang Dacheng Calcium Industry Co., Ltd. were used as space-holders and commercial ZL102 alloy was selected as matrix materials. The main steps of the procedure are: (1) preparation of $CaCl_2$ preforms with different packing densities; (2) infiltration of the preforms with aluminum melt; (3) removal of the $CaCl_2$ preforms. Figure 2 shows the hot-pressing process of $CaCl_2$ particles. 50 g of $CaCl_2$ particles were placed in a steel mould (55 mm in internal diameter) and vibrated to realize preliminary compaction and then hot pressed for 1 h at 60 kPa and 700 °C in a resistance furnace. The steel rod can move down freely because of the hot-deformation of $CaCl_2$ particles during the hot-pressing; it also can be limited to a certain height with the assistance of a locating ring associated with a fastening element. Compression ratios [$\alpha=(h_0-h_1)/h_0$] of $CaCl_2$ preforms of 8%, 15%, 22%, 30% and 40% were obtained precisely by adjusting the height position of the locating ring, where h_0 and h_1 represent the initial and processed height of the preform, respectively. As a result, $CaCl_2$ preforms with different packing densities were obtained. Open-cell aluminum foams were prepared by infiltrating molten Al alloy into these $CaCl_2$ preforms followed by the dissolution of $CaCl_2$ in ingot, which is schematically shown in Fig. 3. The ZL102 ingot was placed on the top of the $CaCl_2$ preform in a crucible placed in the chamber of the furnace. In this work, the process includes two main steps, one is alloy melting under vacuum condition, as illustrated in Fig. 3(a), the other is melt infiltration with high-pressure gas, as shown in Fig. 3(b). Prior to melting, the vacuum pump was first started, then preforms were heated to 700 °C under vacuum for 2 h to ensure the molten of the Al block. Once the liquid sealing was formed, preforms were infiltrated by the aluminum melt using applied gas (Ar) pressure (2 bar). The resulting Al-$CaCl_2$ composite was then solidified, extracted from the crucible and machined to the desired dimension prior to the removal of $CaCl_2$ in distilled water, leaving an open-pore aluminum foam. To improve the reliability of the experiment, three preforms were prepared for each condition.

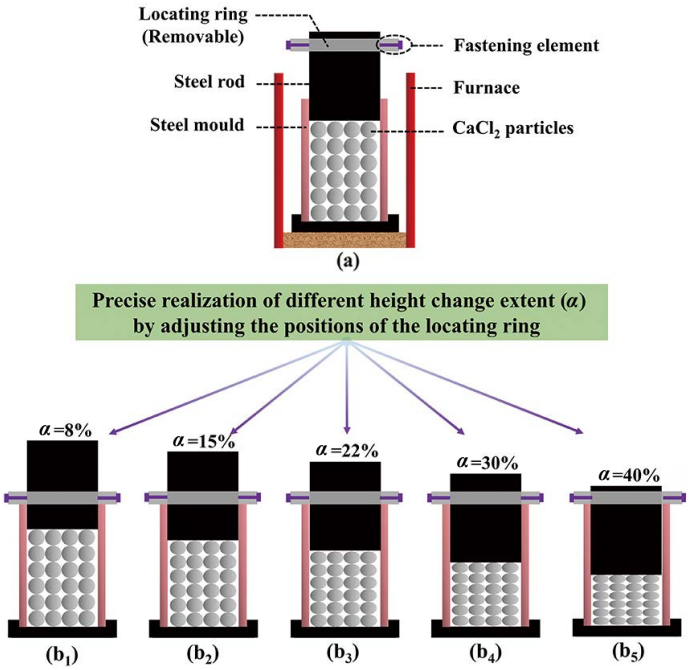

Fig. 2: Preparation of $CaCl_2$ preforms: (a) hot-pressing system; (b_1)-(b_5) preforms with 8% to 40% compression ratios

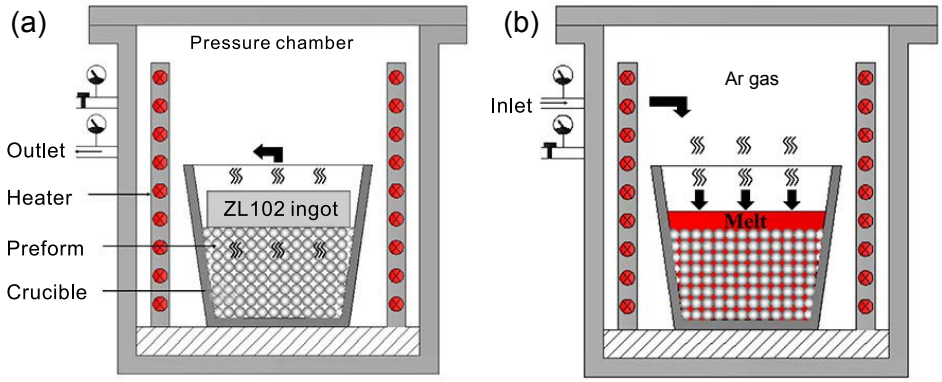

Fig. 3: A schematic illustration of infiltration process for aluminum foam preparation: (a) alloy melting under vacuum condition; (b) melt infiltration with high-pressure gas

2.2 Structural characterization

The structures of $CaCl_2$ preforms and open-cell aluminum foams were observed by an optical microscope, and the pore characteristic of aluminum foam was analyzed by Image-Pro software. Porosity (P) of the foams was determined by the following equation:

$$P = (1 - \rho_0 / \rho_S) \quad (2)$$

where ρ_0 is the apparent density of the foam determined by its dimension and weight, and ρ_S is the density of ZL102 alloy.

Figure 4 shows the optical morphologies of $CaCl_2$ preforms prepared by hot-pressing for different compression ratios. It shows that $CaCl_2$ particles can be successfully sintered into a preform, indicating that there are bonded zones between the contacted particles which benefited from hot-pressing sintering [31]. $CaCl_2$ particles are tighter when increasing the compression ratio, and deform noticeably along the hot-pressing direction, meaning a higher packing density of preform is achieved successfully by precision hot-pressing [32].

As well as changing the packing density of the $CaCl_2$ preform, precision hot-pressing treatment can also influence the character of the particle-particle contact point. The contact area of the neighboring $CaCl_2$ granules is increased with an increase in deformation ratio, which is displayed by black circles containing typical structures of three stacking $CaCl_2$ particles in Fig. 4.

Previous research has indicated that $CaCl_2$ granules are easy to suffer from deformation at a temperature of 700 °C and a pressure of 60 kPa in a short time, resulting in the densification of $CaCl_2$ preforms [17]. The above phenomenon is also observed in our experiment. However, different from the deformation controlled by holding time, pressure or temperature, precision deformation can be realized by a locating ring used for adjusting the height of the steel rod (providing pressure). The pressure will be released automatically once the locating ring touches the mould edge, leading to the end of the hot-pressing treatment and the shaping of the treated preforms. At a small previously set deformation, insufficient sintering dominated by atomic diffusion appears because of a short time of hot-pressing, causing weak bonding between some particles, as shown in Figs. 4(a) and (b). As the deformation increases, there is more time and space for hot-pressing. Accordingly, these $CaCl_2$ particles become much more compact and stably bonded, benefiting to the increasing of both packing density of the preform and contact area between adjacent particles [33]. Aluminum foams processed from these preforms would possess different corresponding structures, mainly containing porosity and channel size.

Figure 5 shows the macrographs taken along the surface of aluminum foams prepared with different compression ratios of 8% to 40% and the same infiltration pressure of 2 bar. As can be seen in Fig. 5, the pores evolving from the $CaCl_2$ particles are interconnected to their neighbors via channels originating from the contact surface between the neighboring $CaCl_2$ granules. Table 1 provides the detailed values of porosity and channel size for each aluminum foam. Porosity varies from 63.1% to 87.3%, and the channel size varies from 0.2 to 1.6 mm. Judging from Fig. 5 and Table 1, it is found that when deformation increases, the foam exhibits higher porosity, thinner cell wall, and larger channels. The difference between the five samples is in accordance with the packing densities of the preforms that are precisely controlled by the location of the locating ring.

3 Compressive behavior of open-cell aluminum foams

3.1 Mechanical performance

The compression test for the resultant foams was performed in a minicomputer-controlled electronic universal testing system (model AGS-J) at the strain rate of 1.7×10^{-3}. The compression test specimens with dimensions of 30 mm×30 mm×30 mm and with different porosities were cut from the center of aluminum foams via a wire-cut machine. A total of five specimens were tested at room temperature.

Figure 6 shows the compressive stress-strain curves of aluminum foam samples with different porosities, where ε is the nominal strain and σ is the nominal stress. It can be observed from Fig. 6 that all the aluminum foams show conventional metallic foam behavior including three distinct

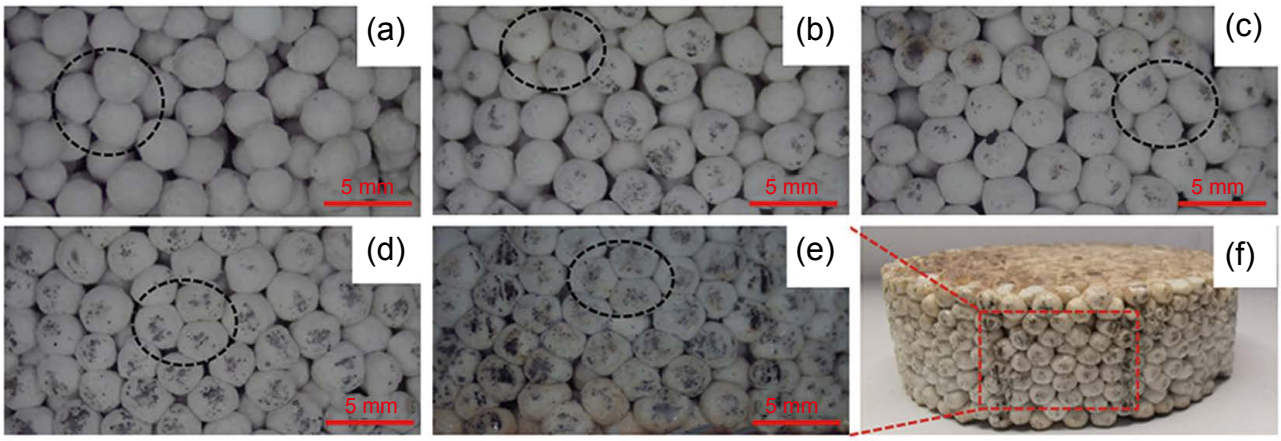

Fig. 4: $CaCl_2$ preforms formed by hot-pressing: (a)–(e) preforms compressed to different degrees (8%, 15%, 22%, 30%, 40%); (f) optical image of $CaCl_2$ preform compressed by 40%

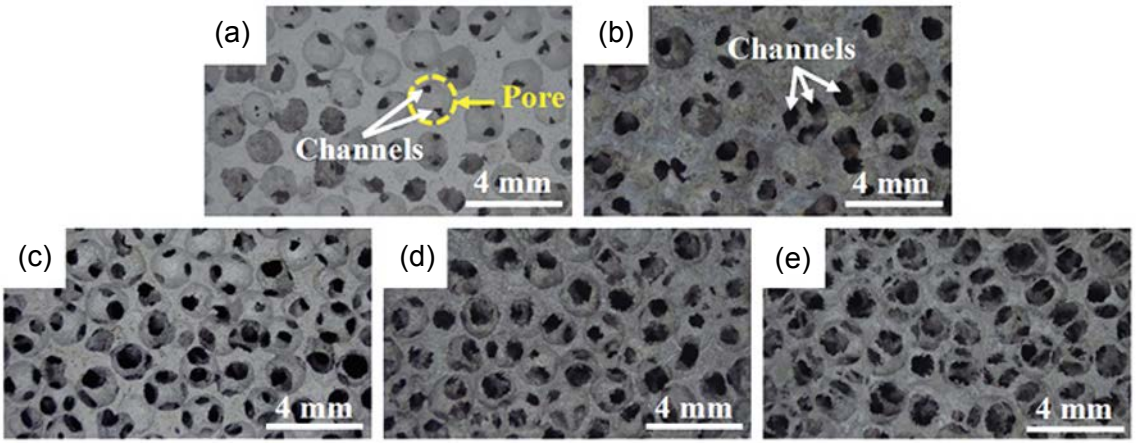

Fig. 5: Morphologies of open-cell aluminum foams processed with $CaCl_2$ preforms compressed by 8% to 40% (a–e)

stages: linear elasticity at the beginning followed by a long plateau region, truncated by densification stage during which the stress rises steeply with strain. As the porosity increases, the curves display three apparent changes: first, lower plateau region appears, which announces the drop of plateau stress; second, the length of plateau region gets longer, which means the densification stage arrives later; third, the elastic region becomes smoother, which indicates lower elastic modulus. In addition, the stress during the plateau stage increases with the strain, which is inconsistent with the Gibson and Ashby's model, in which the stress keeps constant during this stage. For foams with low porosities, this strain-hardening phenomenon becomes more obvious.

Table 1: Structural parameters of aluminum foams

Sample No.	#1	#2	#3	#4	#5
α (%)	8	15	22	30	40
Channel size (mm)	0.3±0.1	0.6±0.2	0.7±0.2	0.8±0.3	1.1±0.5
Porosity (%)	63.1	69.1	74.3	81.5	87.3

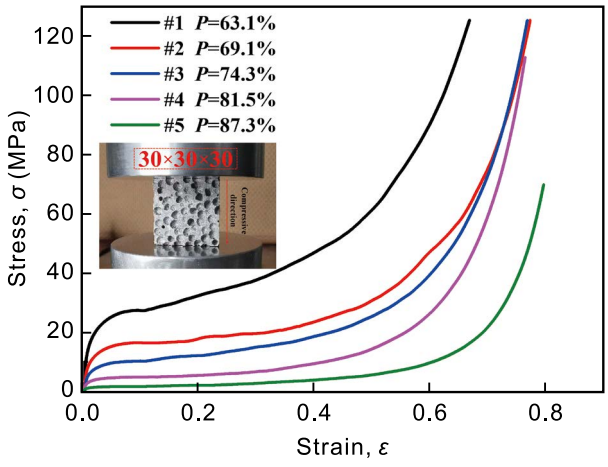

Fig. 6: Compressive stress-strain curves of aluminum foams with different porosities

It is widely acknowledged that porosity plays a major role in the mechanical performance of the foam. Those foams prepared by the space-holder technique associated with spherical $CaCl_2$ particles have homogeneous and controllable structures. Unlike the ALPORAS route [34] for the fabrication of closed-cell foams, the porosity and pore size are two entirely independent parameters and can be controlled separately without interaction with each other. More importantly, the application of precision hot-pressing provides an effective way to achieve stepless adjustment of porosity. It is therefore more convenient and direct to study the effect of porosity on the compressive behavior of aluminum foams without the interruption of pore size.

Figure 7 shows the effect of the aluminum foam's porosity on the mechanical performance, and detailed performance data are summarized in Table 2. The variation of elastic modulus E_0 as a function of porosity P is presented in Fig. 7(a), in which E_0 is measured by linear regression of the initial elastic linear region on the quasi-static compressive σ-ε curve. The variation of plateau stress σ_p as a function of P is given in Fig. 7(b), in which σ_p is obtained by calculating the average stress of the plateau region as follows [28]:

$$\sigma_p = \frac{\int_{\varepsilon_y}^{\varepsilon_d} \sigma(\varepsilon)\mathrm{d}\varepsilon}{\varepsilon_d - \varepsilon_y} \approx \frac{\int_0^{\varepsilon_d} \sigma(\varepsilon)\mathrm{d}\varepsilon}{\varepsilon_d} \tag{3}$$

where ε_d and ε_y are the densification strain and yield point in the σ-ε curve, where ε_y is negligibly small, and ε_d is calculated as following [28]:

$$\eta(\varepsilon) = \frac{\int_0^{\varepsilon} \sigma(\varepsilon)\mathrm{d}\varepsilon}{\sigma(\varepsilon)} \tag{4}$$

$$\frac{\mathrm{d}\eta(\varepsilon)}{\mathrm{d}\varepsilon}\Big|_{\varepsilon=\varepsilon_d} = 0 \tag{5}$$

where η is the energy absorption efficiency during the compression. As seen from Fig. 7 that both elastic modulus E_0 and plateau stress σ_p can be described as power functions of porosity P and they grow monotonously with P, which is consistent with Gibson and Ashby model [23].

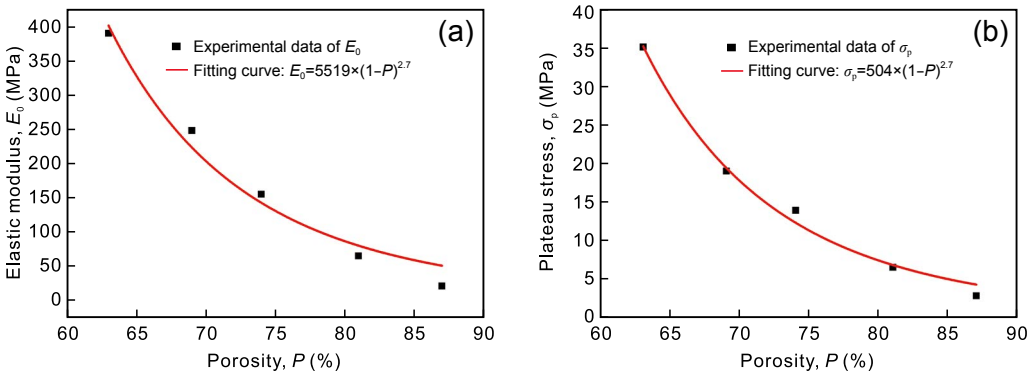

Fig. 7: Influence of porosity P on elastic modulus E_0 (a) and plateau stress σ_p (b)

Table 2: Mechanical performances of aluminum foams

Sample No.	#1	#2	#3	#4	#5
P (%)	63.1	69.1	74.3	81.5	87.3
E_0 (MPa)	389	247	154	64	20
σ_p (MPa)	35.1	19.0	13.9	6.5	2.8

The growth of E_0 and σ_p reveals that the mechanical performance of aluminum foam can be significantly enhanced by reducing the porosity, so that it possesses more solid phases to resist external loads. At the same time, the compressive stress increases with strain during the compression, and the lower the porosity of the foam, the faster the increasing rate because of the dissimilar dominant failure modes for foams with different porosities at the macro level of the cell wall. The compressive stress can remain constant if foam cells are collapsed through forming plastic hinges in Gibson and Ashby's opinion. A plastic hinge will appear when the stress exceeds the yield point of the cell wall on the whole cross-section. Apparently, those foams with thick cell walls require more stress to form plastic hinges under compression. It is easy to form plastic hinges for foams with high porosities because of the thinner cell walls. So, the cells are likely to suffer collapse accompanied with relative rotation of cell walls around the developed hinges [34, 35]. Conversely, for foams with low porosities, it is difficult to form plastic hinges due to the thicker cell walls. The entire cell walls are compressed to collapse under this circumstance, causing an increase in stress. Accordingly, foam with high porosity shows relatively poor mechanical performance and an unobvious strain-hardening phenomenon.

3.2 Energy absorption capacity

3.2.1 Comparison of energy absorption capacity based on strain

As shown in Fig. 6, aluminum foams exhibit many advantages in the field of energy absorption for the long plateau during the plastic deformation stage arising from the continuous cell collapse, which allows large strain at slowly enhanced stress. It is traditional to assess the energy absorption capacity (W) of foams by integrating the compression curve up to a specific strain:

$$W = \int_0^{\varepsilon} \sigma(\varepsilon)\mathrm{d}\varepsilon \tag{6}$$

Figure 8(a) gives the W-ε curves to characterize energy absorption capacity, where W represents the energy absorption capacity equaling to the energy absorption per unit volume during the whole compression test. It can be seen aluminum foam has better energy absorption capacity with low porosity for any given strain.

As mentioned above, the energy absorption capacity of aluminum foams arises from cell collapse by cell's yielding, buckling, crushing, and friction between cell walls while contacting each other. The foams with low porosities exhibit elevated yield and fracture strength compared with those with high porosities [36, 37]. Also, they release more frictional energy during the cell collapse due to a higher volume fraction of the solid matrix in the foams. Hence, foams with lower porosities can absorb more energy than those with high porosities during compression.

Commonly, the energy absorption at densification strain $W\varepsilon_d$ (densification strain energy) is characterized by the energy absorbed at strain ranging from 0 to densification strain ε_d. Figure 8(b) shows the relationship between $W\varepsilon_d$ and P. The densification strain energy decreases as a power function of porosity. Although foam with lower porosity possesses a lower value of densification strain, the value of densification strain energy is higher attributed by the higher plateau stress σ_p.

In some cases of energy absorption, the weight of energy absorbing materials cannot be ignored. In other words, the energy absorption capacity and lightweight of the foam should be considered simultaneously. Here, W_m, the energy absorbed per unit weight by the foam is used to characterize the comprehensive performance of energy absorption:

$$W_m = \frac{1}{\rho_f}\int_0^{\varepsilon} \sigma(\varepsilon)\mathrm{d}\varepsilon \frac{1}{(1-P)\rho_{Al}}\int_0^{\varepsilon} \sigma(\varepsilon)\mathrm{d}\varepsilon \tag{7}$$

where ρ_f and ρ_{Al} are the density of the foam and aluminum.

Apparently, foams with higher porosities show a certain advantage in the weight reduction at the same energy absorption value, thus showing better comprehensive performance of energy absorption.

Figure 8(c) presents the W_m-ε curves of five aluminum foams. It can be seen although the weight of foams is taken into consideration, the energy absorption capacity decreases monotonously with the increasing P on the whole, which shows the similar law in Fig. 8(a).

3.2.2 Comparison of energy absorption capacity based on stress

Although those foams with low porosities can absorb more energy at any given strain, a non-negligible factor of the stress during the energy absorption should be taken into consideration in the practical application of protection [38]. The stress transferred to the protected object should be controlled within a certain level. Namely, protection will be meaningless if damage occurs in the protected component even though enough energy is absorbed. Accordingly, characterization of the energy absorption capacity at the same compressive stress is more suitable than at the same compressive strain for protection application. Figure 9 gives the W-σ curves of the five aluminum foams, which display quite different features compared to W-ε curves in Fig. 8(a). As seen, under the same load stress level, aluminum foams with higher porosities do not always display poor energy absorption capacity, which is quite different from the tendency of W-ε curves, in which the energy absorption capacity drops monotonously with P. It can be seen from Fig. 9 that five sections can be observed with the assistance of intersection points σ_1 to σ_4. Under the condition of $\sigma>\sigma_4$, aluminum foams with lower porosities exhibit the highest energy absorption capacity. When $\sigma_1<\sigma<\sigma_4$, aluminum foams with medium porosities show the best energy absorption capacity. Aluminum foams with higher porosities display the highest energy absorption capacity only when $\sigma<\sigma_1$. This indicates that aluminum foam with optimum porosity obtains the best energy absorption capacity for certain stress. Similarly, for any given foam with certain porosity, there is a stress under which the foam shows the highest energy absorption capacity than foams with any other porosities.

For those idealized energy absorption materials possessing constant plateau stress during the plastic deformation stage, the determination of their optimum service conditions is easy and the plateau stress is just the best choice. However, as has been mentioned before, the strain-hardening phenomenon always occurs especially for foam with low porosity, resulting in the significantly increasing plateau stress. Thus, the foam's optimal service condition for energy absorption is indefinable from W-σ curves.

To determine aluminum foam's optimum service condition, energy absorption efficiency η can be applied [39]. As introduced before, η is the ratio of the absorption of energy to stress σ. There is always a maximum value of η at a certain stress because of the existence of the densification stage, during which the growth of absorbed energy is far slower than the sharp increase in the stress. It is worth noting that the η is proportional to the W at a given stress σ. Thus, at a certain σ, the foam with the highest η will possess the best energy absorption capacity.

Figure 10 presents the η-σ curves of aluminum foams with different porosities. As shown, each foam exhibits a maximum

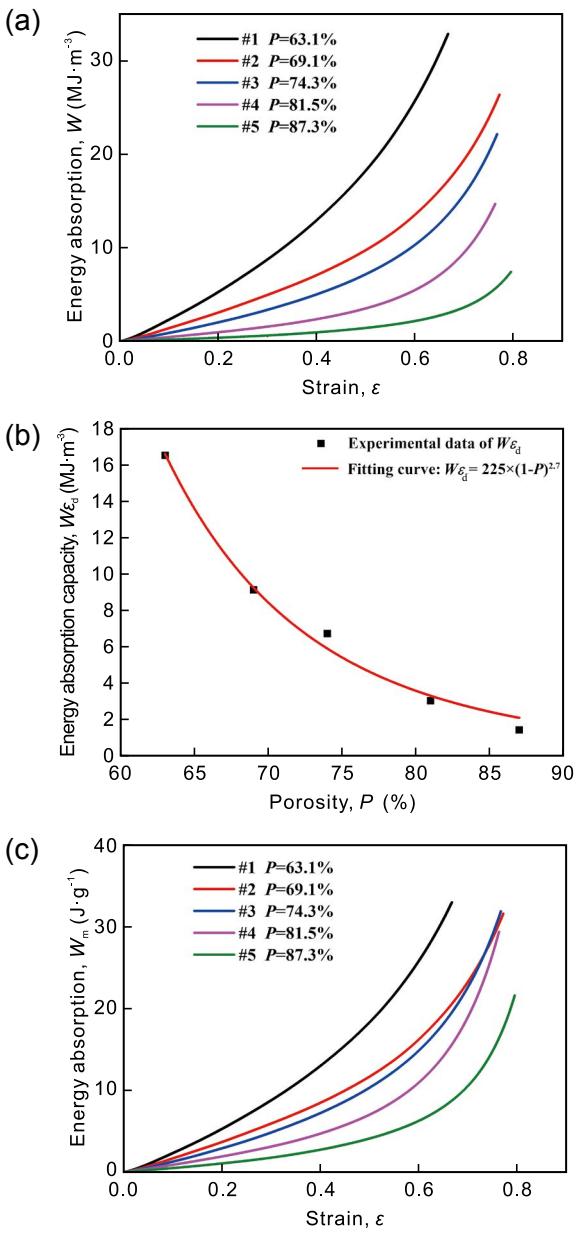

Fig. 8: Curves of aluminum foams at various porosities: (a) energy absorption vs. strain; (b) densification strain energy $W\varepsilon_d$ vs. P; (c) W_m-ε curves

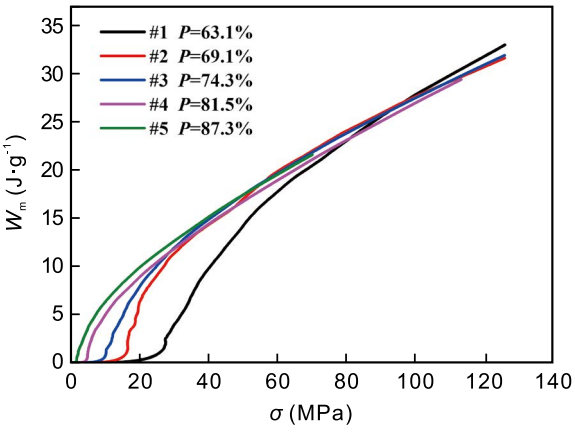

Fig. 9: Comparison of W-σ curves of aluminum foams with different porosities

of η, and the σ corresponding to the maximum value of η decreases with the increase of foam's porosity due to lower stress occurred in the foams with higher porosities during compression. Moreover, the curves can be divided into five parts with the aid of σ_1, σ_2, σ_3 and σ_4, which is the same as the four stress marked in Fig. 9. In each part, there exists one foam showing the highest energy absorption efficiency and thus the highest energy absorption value. Judging from the feature of the curves, the foam presents the highest value of η compared to the foams with any other porosities at the stress determined by its maximum point of η. Accordingly, it owns the best energy absorption capacity W, whose value is equal to $\eta \cdot \sigma$.

Based on the above analysis, aluminum foam's optimum service condition can be determined by the maximum point of η in the η-σ curves. Here, two parameters of optimum operating stress σ_{op} and optimum energy absorption capacity W_{op} are applied to describe the performance of energy absorption. Aluminum foam will show the highest energy absorption capacity W_{op} under the optimum operating stress σ_{op} compared to any other foams with different porosities.

Table 3 gives the σ_{op} and W_{op} of all the five aluminum foams. As shown in Table 3, both the optimum operating stress σ_{op} and optimum energy absorption capacity W_{op} decrease with an increase in the foam's porosity. However, those foams with high porosities show some advantages for weight reduction.

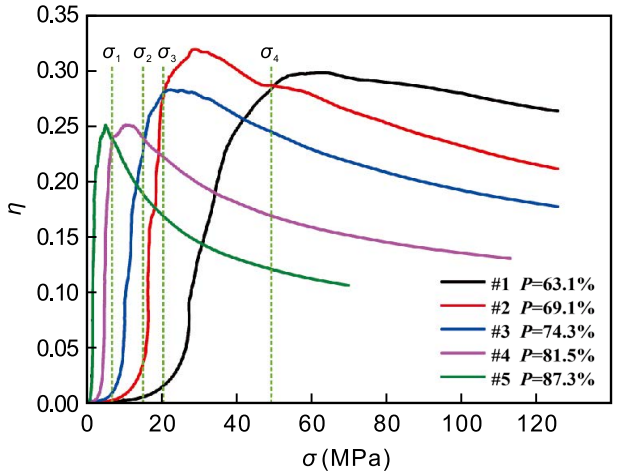

Fig. 10: Comparison of η-σ curves of aluminum foams with different porosities

Table 3: Comparison of optimum operating stress σ_{op} and optimum energy absorption capacity W_{op} of foams with various porosities

Sample No.	#1	#2	#3	#4	#5
P (%)	63.1	69.1	74.3	81.5	87.3
σ_{op} (MPa)	57.3	28.5	21.8	10.5	5.1
W_{op} (MJ·m^{-3})	16.9	9.1	6.5	2.6	1.3

3.3 Design guidelines for energy absorption

Figure 11 shows a composite diagram of σ_{op}-P curve and W_{op}-P curve acquired by fitting the data in Table 3, which can be viewed as a design guide for choosing the foam with optimum porosity P applied in energy absorption.

Energy absorption should be conducted within a certain stress level to protect an object from going through a collision. The certain stress value can be considered as the permissible stress, which apparently is not a constant and depends on the practical situation. Hence, the design guide diagram presented in Fig. 11 can be utilized to select the foam with optimum porosity to act as an energy absorption material at a required permissible stress. Moreover, the optimum energy absorption capacity W_{op} of the corresponding foam can also be obtained from the diagram.

Figure 12 shows the W_m-σ curves of five aluminum foams based on stress. Since the lightweight of energy absorption materials is taken into consideration, the foam with a porosity of 69.1% possesses the highest performance of energy absorption at a wide stress range, which will influence the choice of foam for energy absorption.

As discussed above, aluminum foam with optimum porosity obtains the best comprehensive performance of energy absorption for a certain stress, and the revised energy absorption

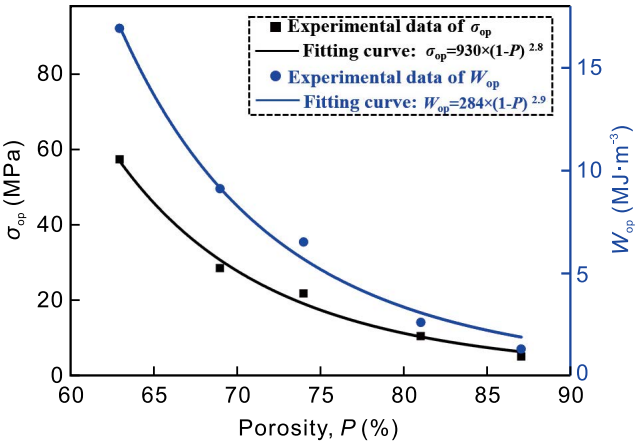

Fig. 11: Design guide diagram for choosing the foam with optimum porosity P applied in energy absorption

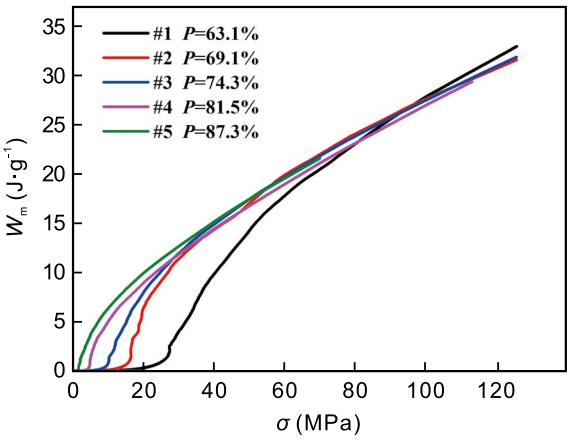

Fig. 12: Comparison of W_m-σ curves of five aluminum foams based on stress

efficiency η' can be used for determining foam's optimum service condition:

$$\eta' = \frac{1}{\rho_f} \cdot \eta = \frac{1}{\rho_f} \frac{\int_0^{\varepsilon} \sigma(\varepsilon) \mathrm{d}\varepsilon}{\sigma(\varepsilon)} \tag{8}$$

similarly, a foam with the highest η' will possess the best comprehensive performance of energy absorption under a certain σ, which can be applied to determine the revised optimum operating stress σ_{op}' and revised optimum energy absorption capacity W_{op}', as same as the determination of σ_{op} and W_{op}. A similar diagram like Fig. 11 for choosing the foam with optimum porosity P applied in energy absorption can also be obtained to be used as design guidance.

4 Conclusions

This study successfully developed the infiltration casting fabrication process based on spherical $CaCl_2$ space-holders. The compressive behavior including the mechanical performance and energy absorption capacity of the fabricated open-cell aluminum foams was investigated systematically. The main conclusions are as follows:

(1) Based on the characteristics that $CaCl_2$ granules can be compressed and deformed at high temperature, the infiltration casting fabrication process based on $CaCl_2$ space-holders can realize the fabrication of open-cell aluminum foams with a wide range of porosities through adjusting the compression ratios of $CaCl_2$ preforms, which can broaden the application fields of open-cell aluminum foams prepared by infiltration casting. Simultaneously, the cell size can remain unchanged and the channel size increases with increasing porosity, which is beneficial to the removing of space-holders.

(2) A strain-hardening phenomenon always occurs especially for open-cell aluminum foams with low porosities at the plateau region, resulting in significantly increasing plateau stress. Moreover, the energy absorption capacity of open-cell aluminum foams decreases with increasing porosity at the same strain. However, at a given stress, each foam can absorb the maximal energy among the five foams in a special stress range.

(3) Open-cell aluminum foam possesses the maximum energy absorption efficiency at its optimum operating stress. At the stress condition, the foam can absorb the highest energy compared with other foams at the same stress point, which provides guidance for the application of energy absorption. The optimum operating stress and corresponding highest energy absorption decrease with increasing porosity. The optimum operating stress for energy absorption can also be determined similarly when the component weight is taken into consideration.

Acknowledgement

This work was financially supported by the National Natural Science Foundation of China (No. 51771101).

References

[1] Banhart J. Manufacture, characterisation and application of cellular metals and metal foams. Progress in Materials Science, 2001, 46: 559–632.
[2] Atwater M A, Guevara L N, Darling K A, et al. Solid state porous metal production: A review of the capabilities, characteristics, and challenges. Advanced Engineering Materials, 2018, 20(7): 1700766.
[3] Wan T, Liu Y, Zhou C X, et al. Fabrication, properties, and applications of open-cell aluminum foams: A review. Journal of Materials Science & Technology, 2021, 62: 11–24.
[4] Garcia-Moreno F. Commercial applications of metal foams: Their properties and production. Materials (Basel), 2016, 9(2): 85.
[5] Kränzlin N,Niederberger M. Controlled fabrication of porous metals from the nanometer to the macroscopic scale. Materials Horizons, 2015, 2(4): 359–377.
[6] Zhou X, Li Y X, Chen X. Development of AlMg35-TiH_2 composite foaming agent and fabrication of small pore size aluminium foams. Journal of Materials Processing Technology, 2020, 283: 116698.
[7] Ding X, Liu Y, Wan T. A novel hot-pressing method to prepare foamable precursor of aluminum foam sandwich (AFS). Materials Letters, 2020, 259: 126895.
[8] Wang N Z, Maire E, Chen X, et al. Compressive performance and deformation mechanism of the dynamic gas injection aluminum foams. Materials Characterization, 2019, 147: 11–20.
[9] Schüler P, Frank R, Uebel D, et al. Influence of heat treatments on the microstructure and mechanical behaviour of open cell AlSi7Mg0.3 foams on different lengthscales. Acta Materialia, 2016, 109: 32–45.
[10] Otaru A J, Morvan H P, Kennedy A R. Measurement and simulation of pressure drop across replicated porous aluminium in the Darcy-Forchheimer regime. Acta Materialia, 2018, 149: 265–273.
[11] Kadkhodapour J, Montazerian H, Samadi M, et al. Plastic deformation and compressive mechanical properties of hollow sphere aluminum foams produced by space holder technique. Materials & Design, 2015, 83: 352–362.
[12] Elizondo L E M, Barari F, Woolley R, et al. Casting protocols for the production of open cell aluminum foams by the replication technique and the effect on porosity. Journal of Visualized Experiments, 2014(94): e52268.
[13] Jia G Z, Hou Y, Chen C X, et al. Precise fabrication of open porous Mg scaffolds using NaCl templates: Relationship between space holder particles, pore characteristics and mechanical behavior. Materials & Design, 2018, 140: 106–113.
[14] Bafti H, Habibolahzadeh A. Compressive properties of aluminum foam produced by powder-Carbamide spacer route. Materials & Design, 2013, 52: 404–411.
[15] Goodall R, Mortensen A. Microcellular aluminium? – Child's play! Advanced Engineering Materials, 2007, 9(11): 951–954.
[16] Chou K S, Song M A. A novel method for making open-cell aluminum foams with soft ceramic balls. Scripta Materialia, 2002, 46(5): 379–382.
[17] Wan T, Liu Y, Zhou C X, et al. Fabrication of high-porosity open-cell aluminum foam via high-temperature deformation of $CaCl_2$ space-holders. Materials Letters, 2021, 284: 129018.
[18] Xu F X, Zhang X, Zhang H. A review on functionally graded structures and materials for energy absorption. Engineering Structures, 2018, 171: 309–325.
[19] Yang X, Cheng Y, He X, et al. Effect of heat treatment on the microstructure, compressive property, and energy absorption response of the Al-Mg-Si alloy foams. Advanced Engineering Materials, 2020: 2000620.

[20] Fan Z Q, Zhang B B, Gao Y B, et al. Deformation mechanisms of spherical cell porous aluminum under quasi-static compression. Scripta Materialia, 2018, 142: 32–35.
[21] Ramamurty U, Paul A. Variability in mechanical properties of a metal foam. Acta Materialia, 2004, 52(4): 869–876.
[22] Jiang B, Wang Z J, Zhao N Q. Effect of pore size and relative density on the mechanical properties of open cell aluminum foams. Scripta Materialia, 2007, 56(2): 169–172.
[23] Gibson L J, Ashby M F. Cellular solids: Structure and properties. 2nd ed., Cambridge: Cambridge University Press, 1997.
[24] Wang H, Fu Y, Su M M, et al. Effect of structure design on compressive properties and energy absorption behavior of ordered porous aluminum prepared by rapid casting. Materials & Design, 2019, 167: 107631.
[25] Xie B, Fan Y Z, Mu T Z, et al. Fabrication and energy absorption properties of titanium foam with $CaCl_2$ as a space holder. Materials Science and Engineering: A, 2017, 708: 419–423.
[26] Fischer S F. Energy absorption efficiency of open-cell pure aluminum foams. Materials Letters, 2016, 184: 208–210.
[27] Cheng H F, Han F S. Compressive behavior and energy absorbing characteristic of open cell aluminum foam filled with silicate rubber. Scripta Materialia, 2003, 49(6): 583–586.
[28] Fan J H, Zhang J J, Wang Z H, et al. Dynamic crushing behavior of random and functionally graded metal hollow sphere foams. Materials Science and Engineering: A, 2013, 561: 352–361.
[29] Jia J G, Jing Y Z, Liu D Q, et al. Compressive properties of porous Cu reinforced by inserting copper pillars or tubes. Journal of Porous Materials, 2021, 28(3): 963–972.
[30] Cheng Y, Li Y X, Chen X, et al. Compressive properties and energy absorption of aluminum foams with a wide range of relative densities. Journal of Materials Engineering and Performance, 2018, 27(8): 4016–4024.
[31] Jinnapat A, Kennedy A. The manufacture and characterisation of aluminium foams made by investment casting using dissolvable spherical sodium chloride bead preforms. Metals, 2011, 1(1): 49–64.
[32] Goodall R, Despois J F, Marmottant A, et al. The effect of preform processing on replicated aluminium foam structure and mechanical properties. Scripta Materialia, 2006, 54(12): 2069–2073.
[33] Hou Y, Jia G Z, Yue R, et al. Synthesis of biodegradable Zn-based scaffolds using NaCl templates: Relationship between porosity, compressive properties and degradation behavior. Materials Characterization, 2018, 137: 162–169.
[34] Cheng Y, Li Y X, Chen X, et al. Fabrication of aluminum foams with small pore size by melt foaming method. Metallurgical and Materials Transactions B, 2017, 48(2): 754–762.
[35] Simone A E,Gibson L J. Effects of solid distribution on the stiffness and strength of metallic foams. Acta Materialia, 1998, 46(6): 2139–2150.
[36] Stanev L, Drenchev B, Yotov A, et al. Compressive properties and energy absorption behaviour of AlSi10Mg open-cell foam. Journal of Materials Science and Technology, 2014, 22(1): 44–53.
[37] Yu S R, Liu J A, Wei M, et al. Compressive property and energy absorption characteristic of open-cell ZA22 foams. Materials & Design, 2009, 30(1): 87–90.
[38] Li W T, Yang X D, He C N, et al. Compressive responses and strengthening mechanisms of aluminum composite foams reinforced with graphene nanosheets. Carbon, 2019, 153: 396–406.
[39] Li Q M, Magkiriadis I, Harrigan J J. Compressive strain at the onset of densification of cellular solids. Journal of Cellular Plastics, 2016, 42(5): 371–392.